6.6: Long-range Electron Transfer in Proteins (Part 1)

Electronic Coupling

The electron-transfer reactions that occur within and between proteins typically involve prosthetic groups separated by distances that are often greater than 10 Å. When we consider these distant electron transfers, an explicit expression for the electronic factor is required. In the nonadiabatic limit, the rate constant for reaction between a donor and acceptor held at fixed distance and orientation is:[70-73]

$$k_{et} = \left[\frac{H_{AB}{}^2}{\hbar} \left(\frac{\pi}{\lambda RT} \right)^{1/2} \right] ^{\frac{-(\lambda + \Delta G^o)^2}{4\lambda RT}} . \tag{6.27}$$

The electronic (or tunneling) matrix element H_{AB} is a measure of the electronic coupling between the reactants and the products at the transition state. The magnitude of H_{AB} depends upon donor-acceptor separation, orientation, and the nature of the intervening medium. Various approaches have been used to test the validity of Equation (6.27) and to extract the parameters H_{AB} and λ. Driving-force studies have proven to be a reliable approach, and such studies have been emphasized by many workers.[73,74]

In the nonadiabatic limit, the probability is quite low that reactants will cross over to products at the transition-state configuration.[72] This probability depends upon the electronic hopping frequency (determined by H_{AB}) and upon the frequency of motion along the reaction coordinate.[75] In simple models, the electronic-coupling strength is predicted to decay exponentially with increasing donor-acceptor separation (Equation 6.28):[72,76]

$$H_{AB} = (H^o_{AB})^{\frac{-\beta}{2}(\mathbf{d}-\mathbf{d}^o)} \tag{6.28}$$

In Equation (6.28), $H_{AB}°$ is the electronic coupling at close contact (**d°**), and β is the rate of decay of coupling with distance (**d**). Studies of the distance dependence of electron-transfer rates in donor-acceptor complexes, and of randomly oriented donors and acceptors in rigid matrices, have suggested $0.8 \leq \beta \leq 1.2$ Å^{-1}.[73,74,77,78]

Analysis of a large number of intramolecular electron-transfer rates has suggested a β value of 1.4 Å^{-1} for protein reactions (Figure 6.24).[79,80] Assigning a single protein β implies that the intervening medium is homogenous. At best this is a rough approximation, because the medium separating two redox sites in a protein is a heterogenous array of bonded and nonbonded interactions.[81-86] Beratan and Onuchic have developed a formalism that describes the medium in terms of "unit blocks" connected together to form a tunneling pathway.[84-86] A unit block may be a covalent bond, a hydrogen bond, or a through-space jump, each with a corresponding decay factor. Dominant tunneling pathways in proteins are largely composed of bonded groups (e.g., peptide bonds), with less favorable through-space interactions becoming important when a through-bond pathway is prohibitively long (Figure 6.25).[84] The tunneling pathway model has been used successfully in an analysis of the electron-transfer rates in modified cytochromes c (Section IV.D.1).

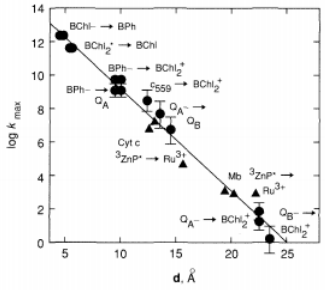

Figure 6.24 - Maximum electron-transfer rate (k_{max}) vs. edge-to-edge distance (**d**) for proteins. Photosynthetic reaction center rates are shown as circles and ^{3}ZnP* to Ru^{3+} rates in modified myoglobins and cytochromes c are shown as triangles. Adapted from Reference 80.

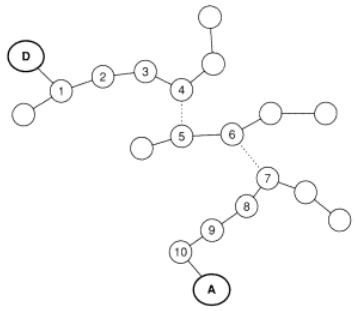

Figure 6.25 - Example of a tunneling pathway.[79] The donor is coupled to the bonded pathway through bond 1 and the acceptor through bond 10. There are three bonded segments and two through-space jumps (between orbitals 4 and 5 and between orbitals 6 and 7).

1. Binding Sites on the Plastocyanin Molecular Surface

Plastocyanin cycles between the Cu^{II} and Cu^{I} oxidation states, and transfers electrons from cytochrome f to the P_{700} component of photosystem I in the chloroplasts of higher plants and algae.[87-89] The low molecular weight (10.5 kDa) and availability of detailed structural information[90] have made this protein an attractive candidate for mechanistic studies, which, when taken together,[87,91-94] point to two distinct surface binding sites (i.e., regions on the plastocyanin molecular surface at which electron transfer with a redox partner occurs). The first of these, the solvent-exposed edge of the Cu ligand His-87 (the adjacent site A in Figure 6.26), is ~6 Å from the copper atom and rather nonpolar. The second site (the remote site R in Figure 6.26) surrounds Tyr-83, and is much farther (~15 Å) from the copper center. Negatively charged carboxylates at positions 42-45 and 59-61 make this latter site an attractive one for positively charged redox reagents.

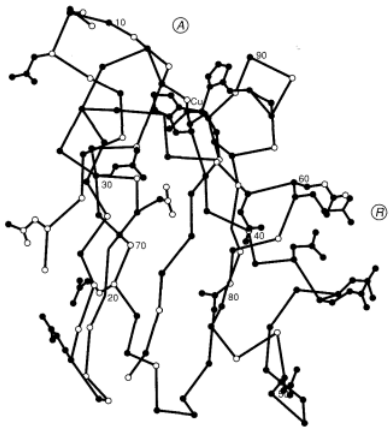

Figure 6.26 - Structure of poplar plastocyanin illustrating the adjacent (A) and remote (R) surface binding sites.

Bimolecular electron-transfer reactions are typically run under pseudo-first-order conditions (e.g., with an inorganic redox reagent present in ~15-fold excess):

$$Rate = k[plastocyanin][complex] = k_{obs}[plastocyanin]. \tag{6.29}$$

For some reactions [e.g., $Co(phen)_3^{3+}$ oxidation of plastocyanin (Cu^{I})] the expected linear plot of k_{obs} vs. [complex] is not observed. Instead, the rate is observed to saturate (Figure 6.27).[95] A "minimal" model used to explain this behavior involves the two pathways for electron transfer shown in Equation (6.30).

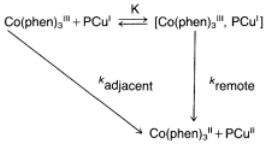

(6.30)

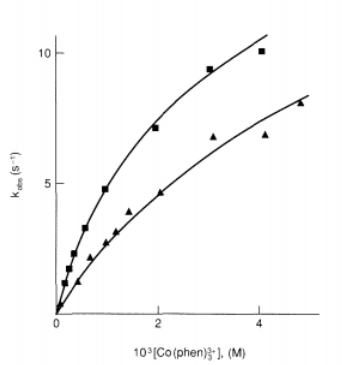

Figure 6.27 - Dependence of first-order rate constants kobs (25 °C) on [$Co(phen)_3^{3+}$] for the oxidation of plastocyanin PCu^I at pH 7.5. Key: ■, *spinach; and* ▲, *parsley.*[95]

Surprisingly, the rate ratio $k_{remote}/k_{adjacent}$ is 7.

Calculations[81] indicate that, despite the significant differences in distances, H_{AB} for the remote site is ~15 percent of H_{AB} for the adjacent site. This figure is much higher than would be expected from distance alone, suggesting that the value of the decay parameter β in Equation (6.28) depends strongly on the structure of the intervening medium.

Modified Metalloproteins

Chemical modification of structurally characterized metalloproteins by transition-metal redox reagents has been employed[52,53,96-98] to investigate the factors that control long-range electron-transfer reactions. In these semisynthetic multisite redox systems, the distance is fixed, and tunneling pathways between the donor and acceptor sites can be examined.

1. Ruthenium-modified Myoglobin

Sperm-whale myoglobin can be reacted with $(NH_3)_5Ru(OH_2)^{2+}$ and then oxidized to produce a variety of ruthenated products,[52,99-101] including a His-48 derivative whose Ru ↔ Fe tunneling pathway is depicted in Figure 6.28.

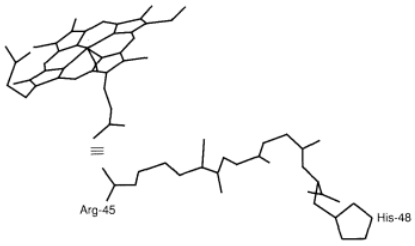

Figure 6.28 - Electron-tunneling pathway for myoglobin modified at His-48. The pathway moves along the protein backbone from His-48 to Arg-45, and then to the heme via an H-bond (=) to the heme propionate. The His-48 to heme edge-edge distance is 12.7 Å.[101]

Electrochemical data (Table 6.5) indicate that the $(NH_3)_5Ru^{3+}$ group does not significantly perturb the heme center, and that equilibrium (i.e., $k_{obs} = k_1 + k_{-1}$) should be approached when a mixed-valent intermediate is produced by flash-photolysis techniques:

$$(NH_3)_5Ru^{3+} - Mb(Fe^{3+}) \xrightarrow[e^-]{fast} (NH_3)_5Ru^{2+} - Mb(Fe^{3+}) \underset{k_{-1}}{\overset{k_1}{\rightleftharpoons}} (NH_3)_5Ru^{3+} - Mb(Fe^{2+}) \qquad (6.31)$$

This kinetic behavior was observed,[52] and both the forward (k_1) and reverse (k_{-1}) reactions were found to be markedly temperature-dependent: $k_1 = 0.019\ s^{-1}$ (25 °C), $\Delta H_1^{\ddagger} = 7.4$ kcal/mol, $k_{-1} = 0.041\ s^{-1}$) (25°C), $\Delta H_1^{\ddagger} = 19.5$ kcal/mol. X-ray crystallographic studies[102] indicate that the axial water ligand dissociates upon reduction of the protein. This conformational change does not control the rates, since identical results were obtained when a second flash-photolysis technique[99] was used to generate $(NH_3)_5Ru^{3+}$-$Mb(Fe^{2+})$ in order to approach the equilibrium from the other direction.

Table 6.5 - Thermodynamic parameters for the reduction of $(NH_3)_5Ru^{3+}$ and the heme site in native and modified myoglobin (Mb).[a]

a) pH 7.0 μ = 0.1 M phosphate buffer.

Thermodynamic Parameter	Native Mb $Fe^{3+/2+}$	Modified Mb	
		$Fe^{3+/2+}$	$(NH_3)_5Ru^{3+/2+}$
E°, mV vs. NHE (25 °C)	58.8 ± 2	65.4 ± 2	85.8 ± 2
Δ G°, kcal mol^{-1} (25 °C)	-1.26 ± 0.05	-1.51 ± 0.05	-1.98 ± 0.05
ΔS°, e.u.	-39.2 ± 1.2	-37.6 ± 1.2	4.2 ± 1.2
ΔH°, kcal mol^{-1} (25 °C)	-13.0 ± 0.4	-12.7 ± 0.4	-0.7 ± 0.4

Cyanogen bromide has been used[103] to modify the six-coordinate metmyoglobin heme site, causing the coordinated water ligand to dissociate. The CNBr-modified myoglobin heme site is thus five-coordinate in *both* oxidation states. As expected, the self-exchange rate increased from ~1 $M^{-1}s^{-1}$ to ~10^4 $M^{-1}s^{-1}$.

Recent efforts in modeling biological electron transfers using chemically modified redox proteins[104-106] point the way toward the design of semisynthetic redox enzymes for catalytic applications. An intriguing example, termed flavohemoglobin, was produced by reaction of hemoglobin with a flavin reagent designed to react with Cys-93 of the β-chain (i.e., the hemoglobin molecule was modified by two flavin moieties).[107] The resulting derivative, unlike native hemoglobin, accepts electrons directly from NADPH and catalyzes the *para*-hydroxylation of aniline in the presence of O_2 and NADPH.

Protein-protein Complexes

In physiologically relevant precursor complexes, both redox centers are frequently buried in protein matrices. Characterization of such protein-protein complexes is clearly important, and several issues figure prominently:

1. What are the "rules" that govern complex formation? How important are protein-dipole/protein-dipole interactions, intermolecular hydrogen bonding, and hydrophobic interactions?
2. Are the water (and small solute) molecules associated with protein surfaces "squeezed" out of the interfacial region upon complex formation?
3. Within a given complex, is there a high degree of structural order, or do the proteins retain some independent mobility?

Most of our knowledge about the structures of protein-protein complexes comes from crystallographic studies[108-110] of antigen-antibody complexes and multisubunit proteins; such systems generally exhibit a high degree of thermodynamic stability. On the other hand, complexes formed as a result of bimolecular collisions generally are much less stable, and tend to resist attempts to grow x-ray-quality crystals; the high salt conditions typically used in protein crystallizations often lead to dissociation of such complexes.

1. Cytochrome b_5-cytochrome c

One of the most widely studied protein-protein complexes is that formed between mammalian cytochrome b_5 and cytochrome c. Using the known x-ray structures of both proteins, Salemme[111]generated a static computer graphics model of this electron-transfer complex by docking the x-ray structures of the individual proteins. Two features of this model and its revision[112] by molecular dynamics simulations (Figure 6.29 See color plate section, page C-12.) are noteworthy: (1) several Lys residues on cytochrome c and carboxylate-containing groups on cytochrome b_5 form "salt bridges" (i.e., intermolecular hydrogen bonds); and (2) the hemes are nearly coplanar and are ~17 Å (Fe-Fe) apart. This distance was confirmed by an energy-transfer experiment[113] in which the fluorescence of Zn-substituted cytochrome c was quenched by cytochrome b_5. Spectroscopic studies[114,115] have verified the suggestion that these proteins form a 1:1 complex at low ionic strength (Figure 6.30). In addition, chemical modification[116] and spectroscopic analyses[117-119] are all in agreement with the suggestion[111,112] that the complex is primarily stabilized by electrostatic interactions of the ($-NH_3^+$ ••• ^-O_2C—) type. The effect of ionic strength on the reduction of cytochrome c by cytochrome b_5 is also in accord with this picture:[120] lowering the ionic strength increases the reaction rate, as expected for oppositely charged molecules.

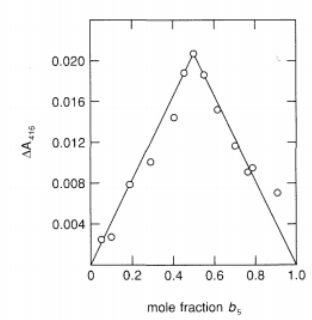

Figure 6.30 - Job plot of the ehange in absorbance at 416 nm due to complex formation between cytochrome b_5 and cytochrome c (25 °C, pH 7.0 (phosphate), μ = 1 mM, 10.54 μM total protein concentration).[114]

2. Hybrid Hemoglobins

A common[52,55,57,121,122] experimental strategy for studying electron transfers *between* proteins uses a metal-substituted heme protein as one of the reactants. In particular, the substitution of zinc for iron in one of the porphyrin redox centers allows facile initiation of electron transfer through photoexcitation of the zinc porphyrin (ZnP). The excited zinc porphyrin, ^{3}ZnP* in Equation (6.32), may decay back ($k_d \sim 10^2$ s^{-1}) to the ground state or transfer an electron to an acceptor.

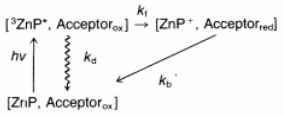

(6.32)

The ZnP^+ cation radical produced in the k_f step is a powerful oxidant; back electron transfer (k_b) will thus occur and regenerate the starting material.

The reactions shown in Equation (6.32) have been investigated in mixedmetal [Zn, Fe] hemoglobins.[123-125] A hemoglobin molecule can be viewed as two independent electron-transfer complexes, each consisting of an α_1-β_2 subunit pair (Figure 6.31), since the α_1-α_2, (\beta_{1}\)-(\beta_{2}\), and α_1-(\beta_{1}\) distances are prohibitively long (> 30 Å).

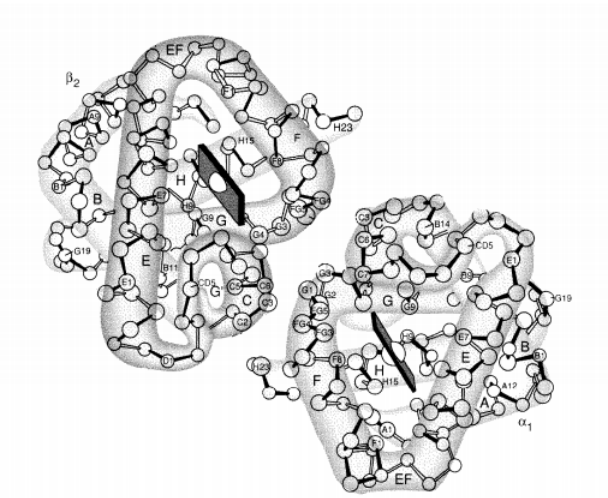

Figure 6.31 - Structure of the α_1 and β_2 subunits of hemoglobin. The edge-edge separation of the two hemes is 20 Å.

Both [α(Zn), β(Fe)] and [α(Fe), β(Zn)] hybrids have been studied. The ZnP and FeP are nearly parallel, as in the cytochrome b_5-cytochrome c model complex. Long-range electron transfer (^{3}ZnP* → Fe^{3+}) between the α_1 and β_2 subunits has been observed (the heme-edge/heme-edge distance is ~20 Å). The driving force for the forward electron-transfer step is ~0.8 eV, and k_f (see Equation 6.32) is ~100 s^{-1} at room temperature, but decreases to ~9 s^{-1} in the low-temperature region (Figure 6.32). Below 140-160 K the vibrations that induce electron transfer "freeze out"; nuclear tunneling is usually associated with such slow, temperature-independent rates. A complete analysis of the full temperature dependence of the rate requires a quantum-mechanical

treatment[126,127] of λ_i rather than that employed in the Marcus theory. It is interesting to note that the heme b vinyl groups (see Figure 6.6) for a given [α_1(Fe), β_2Zn)] hybrid point toward each other and appear[125] to facilitate electron transfer.

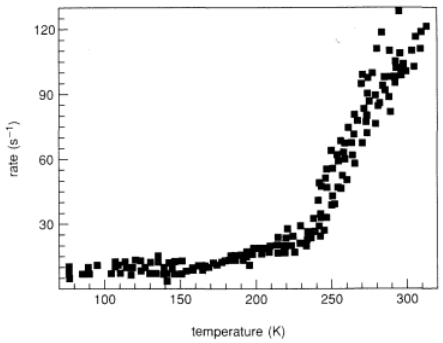

Figure 6.32 - Temperature dependence of the forward electron-transfer rate, k_f, for [α(Zn), β($Fe^{III}H_2O$)]; adapted from Reference 124.